

PACS numbers: 42.25.Dd; 42.65.Re; 42.68.Ay
DOI: 10.1070/QE2006v036n11ABEH013334

Multiple scattering, modulation instability, and filamentation of a femtosecond laser pulse in a dispersion medium

V.O. Militsin, E.P. Kachan, V.P. Kandidov

***Abstract*. Based on the stratified model of multiple coherent scattering of radiation in a dispersion medium, the nonlinear problem of the multiple filamentation of femtosecond laser pulses is studied by the Monte-Carlo method. It is shown that the modulation instability of a high-power light field, which develops on perturbations appearing upon coherent scattering by particles, causes the stochastic breakup of the pulse into numerous filaments. The influence of the size and concentration of particles in water aerosol on the generation of filamentation in a laser pulse is statistically estimated and the regions of different filamentation regimes are determined. The dynamic picture of the evolution of multiple filamentation and formation of plasma channels due to multiphoton ionisation upon aerosol scattering is obtained.**

Keywords: *filamentation, multiple scattering, modulation instability, plasma channel, stratified aerosol model.*

1. Introduction

Investigations of the propagation of high-power femtosecond laser pulses in a real atmosphere attract increasing current interest. This is related to the evolution of femtosecond lasers that can be used for solving a variety of atmospheric problems. These problems include the laser remote sensing of the atmosphere, detection of pollutants in its gas composition and aerosols, control of a breakdown in air for the electric discharge in atmosphere, etc. [1].

The study of the propagation of a high-power femtosecond laser pulse in the atmosphere as a substantially inhomogeneous multicomponent medium [2] is a complex problem. A part of it is the study of the filamentation process, i.e. the spatiotemporal localisation of the laser radiation energy [3 – 5]. Under natural conditions, terawatt laser pulses decompose into numerous random filaments [6] due to the modulation instability of a high-power light field [7]. The instability can develop both at the initial inhomogeneities of the beam [8] and perturbations caused by fluctuations of the refractive index in the atmosphere [9], scattering and absorption of radiation by particles of the atmospheric aerosol [10].

It has been shown in laboratory experiments [11, 12] that the influence of a water aerosol with a high optical density on the filamentation of high-power laser pulses is similar to linear damping. The effect of a dense aerosol, represented in the form of an absorbing layer, on the length of a filament being formed was investigated numerically in [13].

At the same time, the influence of the atmospheric aerosol on the propagation of a femtosecond laser beam is not reduced only to a decrease in its energy. At the laser wavelength considered here ($\sim$ 800 nm), absorption of light in water is negligible. The scattering indicatrix for most particles in the rain and most varieties of clouds and fogs is considerably elongated forward. As a result, the scattered component, which can be strong enough, remains in the beam, by introducing distortions to it. Therefore, multiple coherent scattering of a laser pulse in a aerodispersion medium with parameters typical of atmospheric formations (clouds, fogs, rains) can produce strong perturbations of the light field caused by randomly distributed aerosol particles. Perturbations appearing in the cross section of the pulse can become at a certain critical power the centres of the development of the modulation instability of radiation in a medium with the Kerr nonlinearity [7] and, hence, the regions of the most probable formation of filaments.

The first qualitative results on the filamentation of a laser pulse propagating in a drizzle were obtained in the natural experiment [10]. The formation of a diffraction pattern typical of scattering by spherical particles was observed in the pulse cross section. The numerical studies of filamentation in rain [14] have shown that diffraction perturbations of the intensity caused by scattering by rain drops initiate the stochastic generation of filaments in a high-power femtosecond pulse.

In this paper, we studied the influence of multiply scattered coherent radiation in water aerosol on the development of the modulation instability of laser radiation in air and the formation of numerous filaments in a subterawatt pulse.

2. The stratified model

The propagation of a femtosecond laser pulse in a nonlinear aerosol medium is studied by using the stratified model of light propagation [15]. The model is based on the fact that scattering occurs predominantly forward because the size of particles in atmospheric aerosol formations (clouds, fogs, and rains) considerably exceeds the light

V.O. Militsin, E.P. Kachan, V.P. Kandidov Department of Physics, M.V. Lomonosov Moscow State University, Vorob'evy gory, 119992 Moscow, Russia; e-mail: militsin@ilc.edu.ru, elena.kachan@gmail.com, kandidov@phys.msu.ru

Received 26 July 2006
Kvantovaya Elektronika **36** (11) 1032 – 1038 (2006)
Translated by M.N. Sapozhnikov

wavelength. In this case, backscattering can be neglected and coherent scattering is considered at which interference maxima can be formed, which initiate the generation of filaments due to the modulation instability of the intense light field in air. Note at the same time that a part of the scattered field leaves the beam by reducing its power and, hence, violating the condition for the evolution of self-focusing.

The stratified model simulates an aerodispersion medium by a chain of aerosol screens between which diffraction and nonlinear-optical interaction of a pulse with the gas components of air and the induced laser plasma occurs. Aerosol screens contain particles of a medium by which radiation is coherently scattered, resulting in the redistribution of its intensity in the beam. Thus, the field component scattered by each particle remains in the beam and is then scattered by subsequent screens. Scattering by water particles is analysed by the method of anomalous diffraction [16, 17]. A change in the field $E(t; x, y, z)$ between the screens occurs due to the small-scale self-focusing of the perturbed beam in air and its defocusing in the produced plasma.

Because the size and spatial distributions of aerosol particles are random, the field obtained for a set of screens with randomly distributed drops corresponds to the random field $\tilde{E}(t; x, y, z^*)$ of a single pulse at a specified distance z^*. The statistical characteristics of femtosecond laser radiation in an aerosol medium are determined by the Monte-Carlo method. The ensemble of fields $\tilde{E}_j(t; x, y, z^*)$ $(j = 1, \ldots, M)$ is obtained after repeated simulations of the propagation of pulses in the aerosol medium. In this case, the propagation of each pulse is considered taking into account its scattering by statistically independent chains of aerosol screens.

Analysis is performed in the slowly varying amplitude approximation, which is valid for pulses of duration down to a few cycles of optical oscillations [18]. The model neglects the group-velocity dispersion and a self-steeping effect. These processes affect the pulse variation in time and are important for the full-scale description of the filamentation of laser pulses; however, they are insignificant for the analysis of the initial stage of formation and evolution of pulse filamentation [9]. In the above-mentioned approximation, the equation for the complex field amplitude $E(t; x, y, z)$ can be written in the form

$$2\mathrm{i}k\,\frac{\partial E}{\partial z} = \frac{\partial^2 E}{\partial x^2} + \frac{\partial^2 E}{\partial y^2} + \frac{2k^2}{n_0}\,\Delta n E - \mathrm{i}k\alpha_{\mathrm{ion}} E + \hat{D}_{\mathrm{aer}} E, \quad (1)$$

where k is the wave number corresponding to the wavelength 800 nm; n_0 is the refractive index of air; $\hat{D}_{\mathrm{aer}}$ is the operator describing the field transformation due to coherent scattering by screen particles. The addition Δn to the refractive index is determined by the Kerr nonlinearity Δn_{K} and contribution from the laser-induced plasma Δn_{pl}

$$\Delta n = \Delta n_{\mathrm{K}} + \Delta n_{\mathrm{pl}}, \quad (2)$$

where

$$\Delta n_{\mathrm{K}} = \frac{1}{2}\, n_2 |E|^2; \quad \Delta n_{\mathrm{pl}} = -\frac{2\pi e^2 N_{\mathrm{e}}}{m_{\mathrm{e}}\omega^2};$$

n_2 is the Kerr nonlinearity of the medium; m_{e} and e are the electron mass and charge; and ω is the carrier frequency of radiation. The coefficient α_{ion} describes losses due to multiphoton ionisation:

$$\alpha_{\mathrm{ion}} = \frac{m\hbar\omega}{I(x, y, z)}\,\frac{\partial N_{\mathrm{e}}}{\partial t}, \quad (3)$$

where $I(x, y, z)$ is the light intensity. The values $m = 8$ for oxygen and $m = 10$ for nitrogen determine the number of photons required for the ionisation of molecules of the main gas components of air. Equation (2) neglects the influence of the delay of the nonlinear response caused by stimulated Raman scattering on rotational levels of oxygen and nitrogen molecules. At the initial filamentation stage, this delay leads to the increase in the distance to the beginning of filaments, which can be taken into account by introducing the effective nonlinearity coefficient n_2^{eff} [19].

The electron concentration $N_{\mathrm{e}}(t; x, y, z)$ is determined from the rate equation for multiphoton ionisation [20]

$$\frac{\partial N_{\mathrm{e}}}{\partial t} = R\big(|E|^2\big)(N_0 - N_{\mathrm{e}}), \quad (4)$$

where the ionisation probability $R(|E|^2)$ is specified according to the Perelomov–Popov–Terent'ev model [21]; and N_0 is the concentration of neutral molecules. Equation (4) was solved separately for N_2 and O_2 and the resulting electron concentration N_{e} was determined by taking into account their concentration in air. Equation (4) neglects the contribution of avalanche ionisation because the frequency of collisions of electrons with neutral molecules of air for the field intensity in a filament 10^{13} W cm^{-2} is 6×10^{11} s^{-1} and the probability of inelastic collisions during a femtosecond pulse is negligible.

The model does not consider a change in the optical properties of a water drop during plasma generation inside a particle. As shown in [22], due to focusing upon the refraction of radiation at the spherical boundaries of a drop and reflection from them, a plasma can be formed if the light intensity is two orders of magnitude lower than the photoionisation threshold in pure air. At the same time, reflection from the shadow surface of the drop, which is substantial for the pulse tail, plays a key role in the plasma generation. In addition, the model neglects the influence of particles on the light field of the produced filament. For the filament diameter ~ 100 μm, the probability for a particle to hit the filament is negligibly small. However, both these effects require additional investigations.

The shape of femtosecond pulses is close to a Gaussian [19]. To analyse the influence of coherent scattering in aerosol on filamentation, we will assume that no perturbations of the light field exist in the cross section of the output pulse of a laser. In the approximations adopted above, the amplitude of a collimated pulse incident on an aerodispersion medium can be written in the form

$$E(t; x, y, z = 0) = E_0 \exp\left(-\frac{x^2 + y^2}{2a_0^2}\right) \exp\left(-\frac{t^2}{2\tau_0^2}\right). \quad (5)$$

The numerical simulation was performed by using the calculation grid of size $8a_0 \times 8a_0$ containing 2048×2048 nodes in the pulse cross section. At the grid boundaries, continuously increasing absorption was introduced, which was used to remove from the region under study the field components scattered at a large angle to the propagation direction. The system of equations (1)–(4) in the regions of free propagation of the pulse was solved in the spectral space with the adaptively changing integration step $\Delta z_{\mathrm{nl}}(z)$ in the variable z. The aerosol screens were separated by a

constant step Δz_{aer}. Time integration was performed from $-2.5\tau_0$ to $2.5\tau_0$ on the nonuniform grid with a step that was four times smaller at the pulse centre than at the periphery.

3. Influence of aerosol parameters on the generation of filaments

Perturbations appearing in a dispersion medium upon multiple scattering of radiation by a great number of randomly distributed particles are superimposed, and the generation of filaments occurs stochastically. We will analyse the influence of coherent scattering by water drops on the generation of filaments by considering the initial stage of the process before the production of the laser plasma. Before the achievement of the photoionisation threshold, the power redistribution in a pulse is caused by the Kerr focusing which determines the spatial position of filaments. In this case, nonlinear foci appear in the cross section of the central layer of a pulse with the peak power P_0. Those of them in which the light intensity achieves a photoionisation threshold of 5×10^{13} W cm^{-2} become the centres of filament generation. The distance z at which the photoionisation threshold is achieved in the pulse coincides with the distance at which filaments are generated. Therefore, the initial stage of the formation of filaments is determined by the stationary problem on self-focusing of the central layer of the pulse in aerosol in the absence of plasma nonlinearity.

To study the influence of the particle size on the generation of filaments, we considered the propagation of laser radiation in monodisperse aerosols containing particles of different radii r at the same concentration $n = 10$ cm^{-3}. The average number of particles within a region of radius equal to the radius of the initial beam $a_0 = 2.5$ mm for the stratification layer of thickness $\Delta z_{aer} = 15$ cm was ~ 40. The peak power was $P_0 = 30P_{cr}$ and $100P_{cr}$, where $P_{cr} = 6 \times 10^9$ W is the critical self-focusing power in air [23]. Figure 1 presents the dependence of the maximum intensity I_{max} in the central layer of the pulse on the propagation length z in an monodisperse aerosol. For large particles ($r = 15$ μm) at the pulse peak power $P_0 = 100P_{cr}$, the generation of filaments occurs on average at a smaller distance z than in a medium without particles, while at the peak power $P_0 = 30P_{cr}$ this occurs at a distance that is somewhat larger. Small particles ($r = 2$ μm) at the same concentration almost do not affect the filamentation process; one filament is formed on the pulse axis, which is generated at the same distance as in a medium without particles.

The influence of the size of scattering particles on the generation of filaments depends on the pulse peak power. The obtained dependence is physically explained by the fact that inhomogeneities with the critical self-focusing power appear in a pulse with the peak power $P_0 = 100P_{cr}$ upon scattering by particles of radius $r = 15$ μm. This produces the spatial instability in the beam [7], and initiates nonlinear focusing, resulting in the generation of filaments. As the pulse peak power is decreased down to $P_0 = 30P_{cr}$ or the radius r of scattering particles is reduced, the power accounting for produced perturbations drops below P_{cr}, and no small-scale focusing occurs. In addition, in aerosols with large particles and, hence, with a high optical depth, the radiation energy decreases due to scattering. Atmospheric clouds are a polydisperse aerosol, and large particles play a decisive role in the generation of filaments [15].

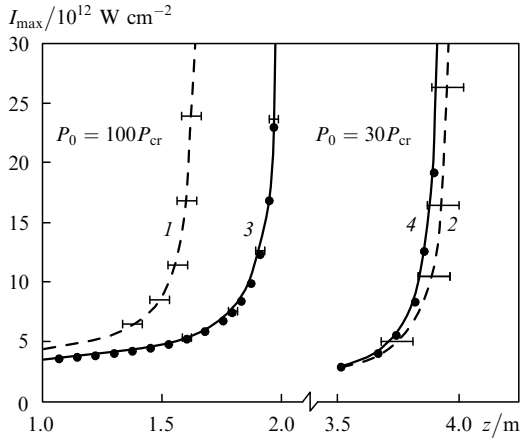

Figure 1. Dependences of the maximum intensity I_{max} in the central layer of a pulse with peak powers $P_0 = 100P_{cr}$ and $30P_{cr}$ on the distance z in a monodisperse aerosol with drops of radius $r = 15$ (*1*, *2*) and 2 μm (*3*, *4*) at the concentration $n = 10$ cm^{-3} and in a medium without particles (points).

We analysed the influence of the concentration of particles on the generation of filaments in a monodisperse aerosol with particles of radius $r = 15$ μm. Figure 2 presents realisations of the intensity distribution $I(x, y)$ at the central layer of the pulse with the peak power $P_0 = 50P_{cr}$ for distances at which the maximum intensity exceeds the initial peak value I_0 by an order of magnitude for different concentrations n of particles. One can see that for $n = 100$ cm^{-3}, several regions containing 'hot points' of high light intensity are observed in the pulse cross section. At higher concentrations, the same increase in the light intensity occurs at a greater distance and the radiation power at 'hot points' considerably decreases. The number of these points and, hence the number of generated filaments also decrease. As the concentration is increased up to 1100 cm^{-3}, the development of small-scale self-focusing ceases along with a general decrease in the light intensity, and radiation power is sufficient only for the formation of one maximum directly on the beam axis. As the concentration and, hence, the optical depth of the aerosol is increased, the pulse power is considerably reduced due to multiple scattering by particles. Thus, at high concentrations both small-scale self-focusing and focusing of the beam as a whole develop slower, resulting in a change in the generation regime of filaments.

A decrease in the radiation power at high concentrations of particles becomes a more important factor than the modulation instability of the light field in a Kerr medium. This is confirmed by the results of statistical tests presented in Fig. 3 demonstrating the dependences of the maximum light intensity in the central layer of the pulse on the distance for different concentrations of particles. Each of the curves is the result of averaging over ten statistically independent realisations of the aerosol path obtained for each concentration.

The curves obtained for low concentrations ($n \sim 50$–300 cm^{-3}) demonstrate that the distance to the onset of formation of filaments is decreased compared to the case of beam self-focusing in a transparent medium (vertical straight line in Fig. 3). This can be explained by the evolution of small-scale self-focusing in the intensity maxima formed due to multiple scattering by drops. At low

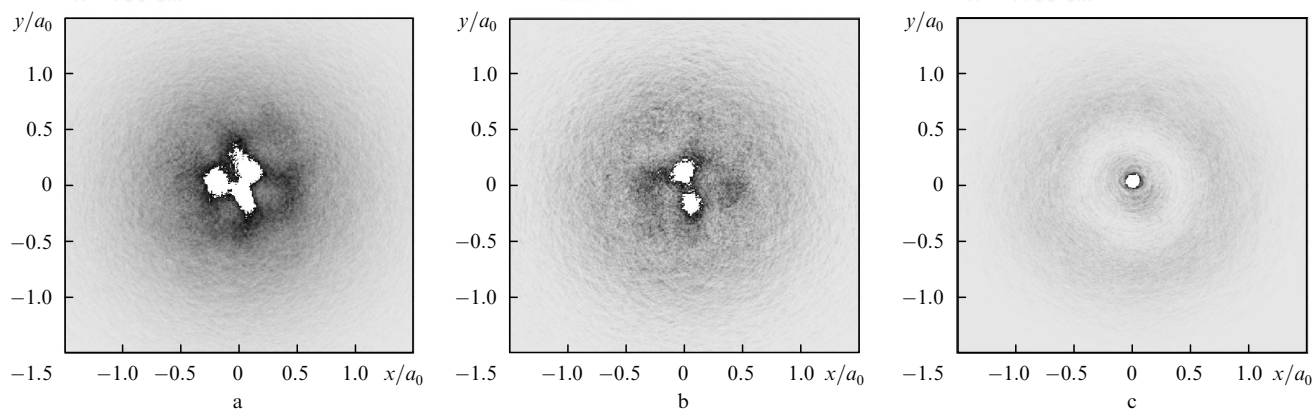

Figure 2. Tone pictures of the random intensity distribution in the central layer of a pulse with the peak power $P_0 = 50P_{cr}$ in a monodisperse medium with drops of radius $r = 15$ μm at concentrations $n = 100$ (a), 500 (b), and 1100 cm^{-3} (c). Distributions are presented for distances for which $I_{max}/I_0 = 10$.

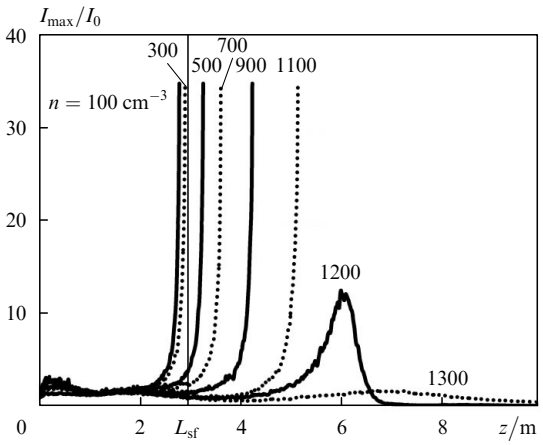

Figure 3. Dependences of the maximum intensity in the central layer of a pulse with the peak power $P_0 = 50P_{cr}$ on the distance z at concentrations n of aerosol particles of radius $r = 15$ μm from 100 to 1300 cm^{-3}.

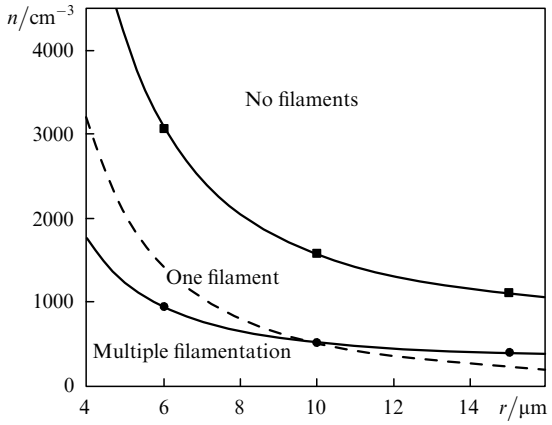

Figure 4. Boundaries of the filament generation regimes for the peak power of a pulse $P_0 = 50P_{cr}$ (solid curves). The dashed curve corresponds to the constant extinction coefficient ($\alpha_{are} = \text{const}$). Points are the numerical experiment.

concentrations of particles, the radiation power localised in high-intensity regions proves to be sufficient for filamentation to occur before the self-focusing of the entire beam. The beam self-focusing length L_{sf} estimated from the Marburger expression [24] is ~ 2.9 m. As the concentration of scattering particles increases, the influence of scattering losses also increases, and filaments are generated at larger distances.

Note that filaments are generated upon a considerable decrease in the beam power as a whole. Thus, at the concentration $n = 900$ cm^{-3}, the optical depth at the distance $z = 4.1$ m, where the peak intensity increases by an order of magnitude, is ~ 5.2. Thus, by the beginning of the plasma production, the radiation energy required for the formation of filaments has scattered considerably and can be insufficient for their further development. If the concentration exceeds 1100 cm^{-3}, the reduction of radiation due to scattering in the aerosol dominates over Kerr self-focusing, the light intensity in the central layer of the pulse does not achieve the photoionisation threshold and no filamentation occurs.

The statistical processing of intensity distributions in the central layer of a high-power laser pulse obtained for monodisperse aerosols with scattering particles of radius $r = 6$, 10, and 15 μm allowed us to distinguish different regimes of formation of filaments. Figure 4 shows the boundaries of three different regimes in the particle concentration – radius plane: multiple filamentation, one filament, and the absence of filamentation for a pulse with the peak power equal to $50P_{cr}$.

Note that the formation of one filament in a pulse with the peak power greatly exceeding the critical self-focusing power in air ($P_0 \gg P_{cr}$) corresponds to the ideal case. Under real conditions, perturbations of the beam profile and fluctuations of the refractive index always exist in the atmosphere and initiate the evolution of several filaments [25].

At the same time, the obtained filamentation boundary of the pulse allows one to estimate quantitatively the expected character of the pulse transformation in an aerosol medium. For the concentration n and radius r exceeding their values corresponding to the boundary of multiple filamentation, the power decrease caused by scattering dominates over the modulation instability of laser radiation. In this case, the filamentation of a pulse in an aerodispersion medium can be analysed by solving the determined problem of the formation of a filament with the linear attenuation α_{aer} instead of the statistical study of the propagation of radiation upon multiple scattering. The formulated determined problem is described by Eqn (1) without the last term determining scattering by particles, and the extinction

coefficient α_{ion} is replaced by the total extinction coefficient

$$\alpha_{\Sigma} = \alpha_{ion} + \alpha_{aer}. \quad (6)$$

The linear extinction coefficient in the aerosol medium is

$$\alpha_{aer} = K_0 \pi r^2 n, \quad (7)$$

where K_0 is the attenuation efficiency for drops of radius r [16]. The results of calculations performed for determined problems of pulse filamentation in homogeneous media with the total extinction coefficient, which is determined by the parameters of monodisperse aerosols, correspond to the diagram in Fig. 4. The dependences of the maximum intensity I_{max} in the pulse cross section on the distance obtained for determined problems coincide within the error with the results of statistical analysis of the generation of one filament or its absence in the aerosol.

Note that the boundaries of filament generation regimes presented in Fig. 4 do not coincide with the contour curves of the extinction coefficient $\alpha_{aer} = \text{const}$ in the dispersion medium. This is illustrated by the dashed curve corresponding to $\alpha_{aer} \approx 0.32$ m^{-1}. One can see that the increase in the particle size at a constant extinction coefficient α_{aer} can result in a passage from the one-filament regime to multiple filamentation. Thus, the aerosol not only attenuates radiation but also produces perturbations of the light intensity, which induce the generation of filaments. The conditions for the formation of such perturbations depend on the scattering indicatrix. As the size of particles is increased, the scattering indicatrix narrows down and the intensity redistribution upon multiple scattering dominated over attenuation. Perturbations produced upon such redistribution initiate small-scale self-focusing in the Kerr medium, resulting in the decrease in the distance to the filamentation onset.

Note that the appearance of even a small number of field perturbations at a low concentration of particles will result, due to modulation instability, in the beam decomposition and generation of numerous filaments. An example is the generation of filaments in a drizzle when the pulse power exceeds the critical self-focusing power by two orders of magnitude [10, 14].

4. Multiple filamentation upon scattering of light in aerosol

The dynamics of filamentation and formation of plasma channels in a femtosecond laser pulse propagating in aerosol described by the system of equations (1)–(3) was considered in the (3D + 1) space of variables. Kinetic equation (3) determining the electron concentration in the plasma was solved at all points of the cross-section plane for each time layer of a pulse during its propagation. We considered a pulse of duration $\tau_0 = 140$ fs with the peak power $P_0 = 50P_{cr}$, which for the pulse diameter $a_0 = 2.5$ mm corresponds to the initial peak intensity $I_0 = 1.5 \times 10^{12}$ W cm^{-2}.

The distance L_{pl} at which the plasma concentration achieves 10^{-3} of the concentration N_0 of neutral molecules can be considered as the distance at which the formation of a plasma channel begins. When a pulse propagates in a transparent medium, one filament is formed on the pulse axis and the plasma concentration achieves the value indicated above at the distance $L_{pl} \approx 2.82$ m. In a monodisperse aerosol with drops of radius $r = 15$ μm at the concentration $n = 100$ cm^{-3}, the plasma formation begins on average at a smaller distance $\langle L_{pl} \rangle \approx 2.76$ m.

Figure 5 presents distributions of the plasma concentration in the pulse cross section at a distance of $z \approx 3.3$ m immediately after the pulse propagation. In the ideal case (Fig. 5b), when random perturbations of the beam profile are absent, the Kerr nonlinearity causes an increase in the light intensity and, hence, the ionisation of the medium only on the pulse axis, while defocusing occurring in the induced plasma restricts this process. As a result, a plasma channel directed along the z axis and restricted in its cross section is formed. Coherent multiple scattering by a stochastic ensemble of particles gives rise to several plasma channels distributed randomly over the beam cross section. The realisation presented in Fig. 5a has three channels, where the electron concentration exceeds $10^{-3}N_0$, and many regions with a lower plasma density, which can either continue to develop with increasing z or disappear due to a complex distribution of the light intensity and a competition between small-scale self-focusing and scattering of radiation by aerosol drops and plasma formations.

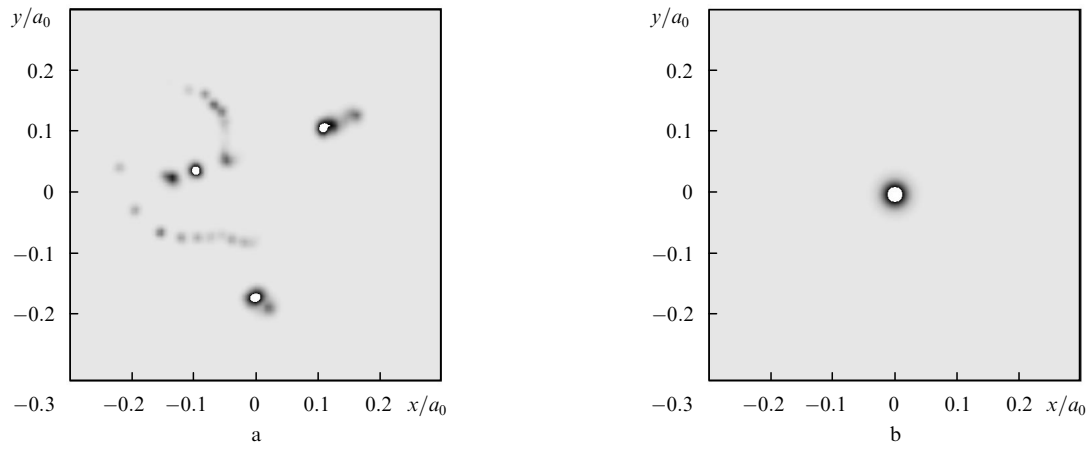

Figure 5. Tone pictures of the distribution of the electron concentration in the cross section of a pulse of duration $\tau_0 = 140$ fs with the peak power $P_0 = 50P_{cr}$ at a distance of $z \approx 3.3$ m in a monodisperse aerosol with particles of radius $r = 15$ μm at the concentration $n = 100$ cm^{-3} (a) and in medium without particles (b).

Note that the distance at which the plasma channel begins to form is close to the average distance at which the maximum intensity of the central layer of the pulse increased by ~ 20 times (Fig. 3). These data confirm the validity of the stationary consideration of the problem of propagation of a high-power femtosecond laser pulse in an aerosol medium for the description of generation of filaments.

The localisation region of plasma formations near the axis of the initial beam is limited on average by the size $0.3a_0 \times 0.3a_0$. The diameter of the high-electron-density region characterising the thickness of plasma channels in the presence of aerosol is a few times smaller than that in a transparent medium. The laser beam energy in the presence of aerosol is less spatially localised and filaments are shorter than upon filamentation of the ideal pulse without distortions.

The volume image of plasma channels in the aerosol presented above (Fig. 5a) is shown in Fig. 6. The surfaces corresponding to the same plasma concentration ($5\times 10^{-4}N_0$) are demonstrated. This picture is the typical example of the regime of multiple filamentation upon propagation of a femtosecond pulse in aerosol. First one plasma channel is formed and then other two channels separated by a large distance appear. These channels are not connected with the first one and are produced due to small-scale focusing of radiation scattered by aerosol particles. Then, secondary plasma channels and separate high-electron-density regions are formed. The local increase in the cross section of the primary plasma channel is explained by refocusing upon pulse filamentation [20]. The formation of the plasma during pulse propagation begins in the temporal layers of the leading edge of the pulse, and the light intensity in them achieves the photoionisation threshold. In this case, the temporal layers of the high-power pulse tail after defocusing in the produced plasma experience repeated self-focusing. As a result, the cross section of the plasma channel increases in the region of pulse refocusing.

A detailed analysis shows that large plasma channels are displaced to the beam axis with increasing the distance. This is explained by the continuation of the Kerr self-focusing of laser radiation as a whole despite the appearance of perturbations in the intensity distribution.

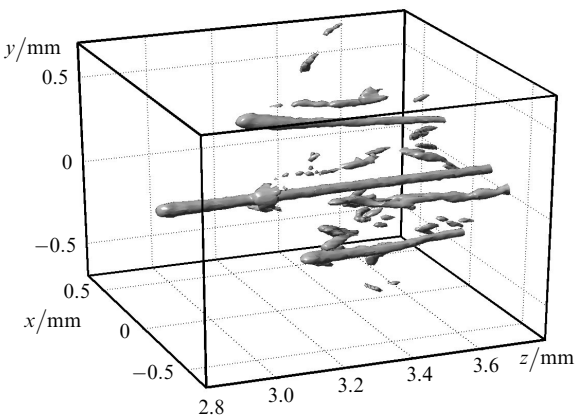

Figure 6. Surfaces corresponding to the same plasma concentration ($5 \times 10^{-4}N_0$) for the typical realisation of propagation of a pulse with the peak power $P_0 = 50P_{cr}$ in a monodisperse aerosol containing particles of radius $r = 15$ μm at the concentration $n = 100$ cm^{-3}.

5. Conclusions

The stratified model of multiple coherent scattering of light by particles allows one to study the development of the modulation instability and, hence, the formation of numerous filaments and plasma channels in a femtosecond laser pulse propagating in an aerodispersion medium. It has been shown that light scattering by particles reduces the pulse power and produces perturbations of the beam intensity initiating its multiple filamentation. The latter dominates over the pulse attenuation if the power producing perturbations is close to the critical self-focusing power in air and the modulation instability of radiation is developed. Such a regime is possible in water aerosol containing particles of radius $r = 15$ μm at the concentration $n < 500$ cm^{-3} for the peak power P_0 exceeding the critical self-focusing power by two orders of magnitude.

Monte-Carlo simulations have shown that the boundaries of different pulse filamentation regimes in the atmospheric aerosol are not determined by the extinction coefficient. As the radius of particles in the aerosol with a constant optical depth is increased, the scattering diagram narrows down, the contribution of multiple scattering increases, the modulation instability of the light field becomes significant, and the probability of multiple filamentation increases.

The numerical analysis of the dynamic filamentation of a high-power femtosecond laser pulse has shown that a stochastic set of extended plasma channels and local regions with a low electron concentration is formed in the water aerosol.

Acknowledgements. This work was supported by the Russian Foundation for basic research (Grant No. 06-02-08004).

References

1. Kasparian J., Rodriguez M., Mejean G., Yu J., Salmon E., Wille H., Bourayou R., Frey S., Andre Y.-B., Mysyrowicz A., Sauerbrey R., Wolf J.-P., Woste L. *Science*, **301**, 61 (2003).
2. Kandidov V.P., Kosareva O.G., Mozhaev E.I., Tamarov M.P. *Opt. Atmos. Okean.*, **13**, 429 (2000) [*Atmos. Ocean. Opt.*, **13**, 394 (2000)].
3. Braun A., Korn G., Liu X., Du D., Squier J., Mourou G. *Opt. Lett.*, **20**, 73 (1995).
4. Nibbering E.T.J., Curley P.F., Grillon G., Prade B., Franco M.A., Salin F., Mysyrowicz A. *Opt. Lett.*, **21**, 62 (1996).
5. Brodeur A., Chien C.Y., Ilkov F.A., Chin S.L., Kosareva O.G., Kandidov V.P. *Opt. Lett.*, **22**, 304 (1997).
6. Berge L., Skupin S., Lederer F., Mejean G., Yu J., Kasparian J., Salmon E., Wolf J.P., Rodriguez M., Woste L., Bourayou R., Sauerbrey R. *Phys. Rev. Lett.*, **92**, 225002.1 (2004).
7. Bespalov V.I., Talanov V.I. *Pis'ma Zh. Eksp. Teor. Fiz.*, **3**, 471 (1966) [*JETP Lett.*, **3**, 306 (1966)].
8. Hosseini S.A., Luo Q., Ferland B., Liu W., Chin S.L., Kosareva O.G., Panov N.A., Akozbek N., Kandidov V.P. *Phys. Rev. A*, **70**, 033802.1 (2004).
9. Shlenov S.A., Kandidov V.P. *Opt. Atmos. Okean.*, **17**, 630 (2004) [*Atmos. Ocean. Opt.*, **17**, 565 (2004)].
10. Mechain G., Mejean G., Ackermann R., Rohwetter P., Andre Y.-B., Kasparian J., Prade B., Stelmaszczyk K., Yu J., Salmon E., Winn W., Schlie L.A., Mysyrowicz A., Sauerbrey R., Woste L., Wolf J.-P. *Appl. Phys. B*, **80**, 785 (2005).
11. Mejean G., Kasparian J., Yu J., Salmon E., Frey S., Wolf J.-P., Skupin S., Vinaotte A., Nuter R., Champeaux S., Berge L. *Phys. Rev. E*, **72**, 026611.1 (2005).

12. Bochkarev N.N., Zemlyanov An.A., Zemlyanov A.A., Kabanov A.M., Kartashe D.V., Kirsanov A.V., Matvienko G.G., Stepanov A.N. *Opt. Atmos. Okean.*, **17**, 971 (2004) [*Atmos. Ocean. Opt.*, **17**, 861 (2004)].
13. Zemlyanov A.A., Geints Yu.E. *Opt. Commun.*, **259**, 799 (2006).
14. Kandidov V.P., Militsin V.O. *Appl. Phys. B*, **83**, 171 (2006).
15. Militsin V.O., Kouzminskii L.S., Kandidov V.P. *Opt. Atmos. Okean.*, **18**, 880 (2005) [*Atmos. Ocean. Opt.*, **18**, 789 (2005)].
16. Zuev V.E., Kabanov M.V. *Optika atmosfernogo aerozolya* (Optics of Atmospheric Aerosols) (Leningrad: Gidrometeoizdat, 1987).
17. van de Hulst H.C. *Light Scattering by Small Particles* (Dover, New York: Wiley, 1957; Moscow: Inostrannaya Lieteratura, 1961).
18. Shpolyanskiy Y.A., Belov D.L., Bakhtin M.A., Kozlov S.A. *Appl. Phys. B*, **77**, 349 (2003).
19. Andrianov K.Yu., Kandidov V.P., Kosareva A.G., Chin S.L., Talebpur A., Petit S., Liu V., Iwasaki A., Nade M.-K. *Izv. Ross. Akad. Nauk, Ser. Fiz.*, **66**, 1091 (2002).
20. Kosareva O.G., Kandidov V.P., Brodeur A., Chin S.L. *J. Nonlinear Opt. Phys. Mater.*, **6**, 485 (1997).
21. Perelomov A.M., Popov V.S., Terent'ev M.V. *Zh. Eksp. Teor. Fiz.*, **50**, 1393 (1966) [*Sov. Phys. JETP.*, **23**, 924 (1966)].
22. Kandidov V.P., Militsin V.O. *Opt. Atmos. Okean.*, **17**, 54 (2004) [*Atmos. Ocean. Opt.*, **17**, 46 (2004)].
23. Nibbering E.T.J., Grillon G., Franco M.A., Prade B.S., Mysyrowicz A. *J. Opt. Soc. Am. B*, **14**, 650 (1997).
24. Marburger J.H. *Prog. Quantum Electron.*, **4**, 35 (1975).
25. Shlenov S.A., Kandidov V.P. *Opt. Atmos. Okean.*, **17**, 637 (2004) [*Atmos. Ocean. Opt.*, **17**, 571 (2004)].